

A novel microelectrostatic torsional actuator

Jerwei Hsieh, Weileun Fang *

Power Mechanical Engineering Department, National Tsing Hua University, Hsinchu, Taiwan

Received 10 August 1998; accepted 7 April 1999

Abstract

Presently, the torsional actuator has gained a lot of attention in the area of microactuators. Because the torsional actuator cannot carry a substantial mechanical load in the out-of-plane direction, it is frequently used in some optical or electrical applications such as light modulators and spatial scanner devices. However, the performance of the torsional actuator is limited to the fabrication process and operating conditions. For instance, it is difficult to fabricate a torsional actuator with both a large rotating angle and large size moving plate. A novel electrostatically driven torsional actuator is proposed in this paper. The torsional actuator is fabricated through the integration of surface and bulk micromachining processes. Thus, the goal of fabricating a torsional actuator with a cavity right beneath the edge of the moving plate is reached. In addition, the thin film residual stress is exploited to modify the shape of the torsional actuator. The advantage of the proposed design is to increase the traveling distance of the actuator as well as to increase the area of the moving plate. In short, the proposed design provides the possibility of increasing the size of a moving plate without reducing its rotating angle. Therefore, the applications for the torsional actuator, such as image scanner and positioner, are increased. © 2000 Elsevier Science S.A. All rights reserved.

Keywords: Torsional actuator; Surface and bulk micromachining

1. Introduction

In general, microelectromechanical systems (MEMS) contain micromechanical structures, microsensors, microactuators, and circuits for signal processing. As a result of the development of microfabrication technology, micromechanical structures and microsensors have attained wide use [1]. The dynamic performances such as response time and sensitivity of a microactuator are better than that of a conventional actuator because of the small size and weight [2]. However, the applications of microactuators are limited by their loading capacity, strength, and traveling range. Presently, microactuators are primarily applied in transmitting such physical quantities as electromagnetic, acoustic, and light energy, instead of force [3–5]. Since the microtorsional actuator is primarily performing out-of-plane angular motion, it is the most common device for the above applications. For example, microtorsional actuators are applied in optical switches [3], light modulators [6],

projection television [7,8], optical choppers [9], optical shutters [10], bar code readers [11], and light positioners [12,13].

The goal of this study is to develop a novel microelectrostatic torsional actuator (META) and improve its performance. A typical META usually consists of the following mechanical components: suspensions, a mirror plate, and electrodes, as shown in Fig. 1. The existing METAs are fabricated through either bulk micromachining [3,4], or surface micromachining [6,14–18]. It is shown in Fig. 1 that the distance between the mirror plate and the electrodes on the substrate d_0 is much larger for a bulk micromachined META. This is due to the cavity etched on the substrate. From Fig. 1, the relationship between the angular deflection of the mirror plate θ , the length of the mirror plate L_p , and the gap between the plate and the substrate d_0 is approximately

$$L_p \theta = d_0. \quad (1)$$

Therefore, a bulk META can be operated with a larger L_p or a larger θ . On the other hand, the driving voltage of a bulk META is greater than a surface META, since the electrostatic force is inversely proportional to d_0^2 . In addi-

* Corresponding author. Tel.: +886-3-574-2923; Fax: +886-3-572-2840; E-mail: fang@pme.nthu.edu.tw

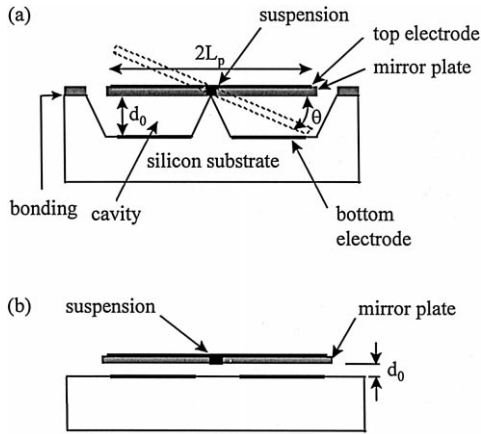


Fig. 1. The existing META fabricated by (a) bulk, and (b) surface micromachining.

tion, the fabrication processes of a bulk META are more complicated due to the requirement for a bonding process. Several techniques had been proposed to improve the performance of the META [4,16,17]. A fabrication technique regarding the deposition of electrodes on the substrate is proposed to prevent the large driving voltage of a bulk META [4]. The angular deflection of the surface META can be increased by introducing special sacrificial layers [16,17].

A novel META fabricated through the integration of surface and bulk micromachining processes is proposed in this paper. The design for unconventional mirror plates and electrodes for the proposed META were also developed. Several design issues regarding the size of the mirror plate L_p , the angular deflection θ , and the driving voltage, will be studied. In short, the proposed META is intended to have an angular deflection as large as a bulk META, yet keep its driving voltage as small as a surface META.

2. Design and analysis

In this section, the design issues regarding the mechanical as well as electrical characteristics of the META will be discussed. The novel META as shown in Fig. 2 is

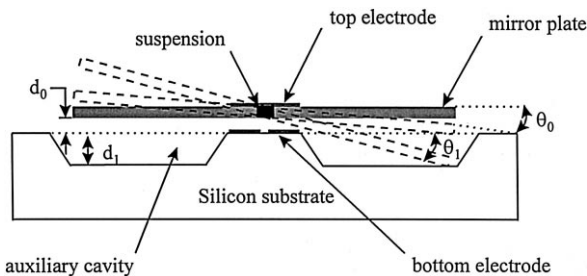


Fig. 2. The proposed META which consists of a surface META and an auxiliary cavity on the substrate.

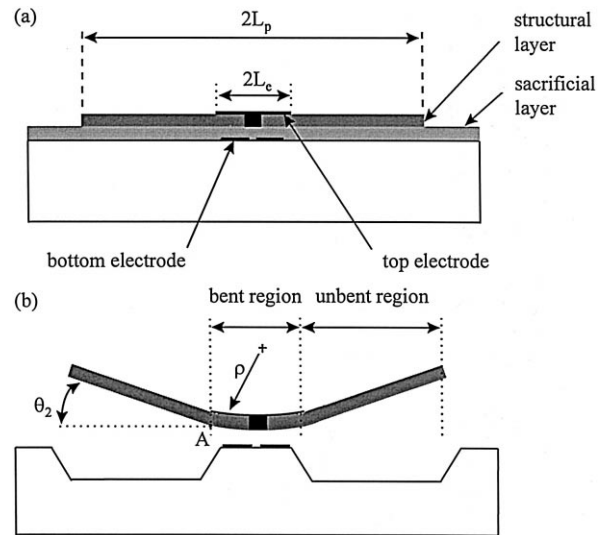


Fig. 3. The proposed META design that contains a partially bent mirror plate (a) before removing the sacrificial layer, and (b) after removing the sacrificial layer.

fabricated through the integration of surface and bulk micromachining. In addition, the residual stress of the thin films is applied to modify the shape of the META. Thus, attributes, such as the angular deflection, plate size, and driving voltage, of the META are improved.

2.1. Surface META with auxiliary cavity

The prototype design of the META proposed in this research is illustrated in Fig. 2. This design consists of a surface META with an auxiliary cavity on the substrate. As indicated in Fig. 2, the gap between the tip of the plate and the substrate is increased from d_0 to $d_0 + d_1$. Therefore, the angular deflection θ_0 , for a given plate length,

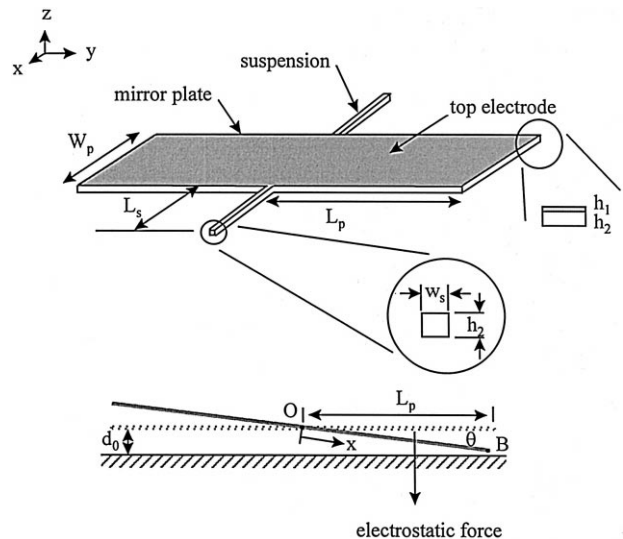


Fig. 4. A straight type suspension.

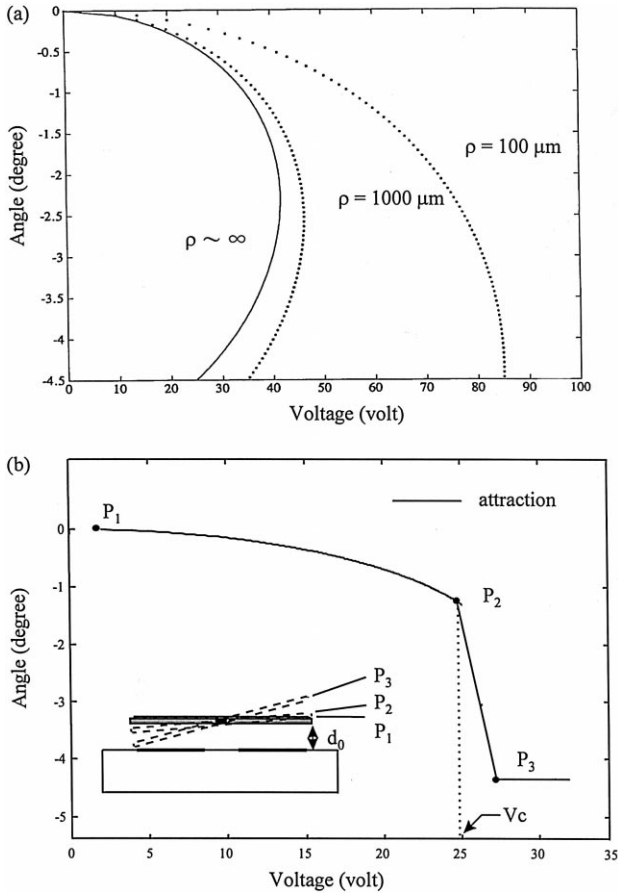


Fig. 5. The characteristic curve between the angular deflection and the driving voltage for (a) idea case from Eq. (5), and (b) real case.

can be increased to $\theta_0 + \theta_1$ from Eq. (1). However, the gap between the middle of the plate and the electrodes on the substrate remains d_0 . Hence, the driving voltage of the META is not increased, since the gap between the driving electrodes is not changed. The details regarding the fabrication processes of the proposed design will be described in Section 3.

2.2. Partially bent mirror plate

According to the fabrication processes, residual stresses always exist in thin film materials [19]. This phenomenon is exploited to fabricate microstructures with desired shapes [20]. A bilayer thin film structure will be bent with a radius of curvature if the residual strains of the two films are different. From Ref. [21], the relationship between the residual strain ε in the film layer and the radius of curvature ρ of the bilayer structure is

$$\frac{1}{\rho} = \frac{6\Delta\varepsilon(1+m)^2}{h \left[3(1+m)^2 + (1+mn) \left(m^2 + \frac{1}{mn} \right) \right]}, \quad (2)$$

where $h = h_1 + h_2$ is the total thickness of the bilayer structure, and $m = E_1/E_2$ and $n = h_1/h_2$ are two nondimensional parameters representing the ratio of values for the elastic constant and thickness, respectively, between the films. Therefore, the radius of curvature of the bilayer structure can be modified by the residual strain of the films through Eq. (2).

In this research, the top electrode with length $2L_e$ is deposited only in the middle region of the mirror plate with a total length $2L_p$, as illustrated by Fig. 3a. Thus, a bilayer structure is formed by the top electrode and the mirror plate. The bilayer region will be bent with a radius of curvature ρ after the sacrificial layer is removed, as illustrated by Fig. 3b. However, the rest of the mirror plate is still flat. Therefore, the mirror plate of the META becomes partially bent, as indicated in Fig. 3b. The flat part of the mirror plate has a tilting angle θ_2 . The angle θ_2 , measured in radian, is formed by the tangent at the tip of the bilayer structure (point A in Fig. 3b) and the horizontal (substrate surface). Consequently, a META with any size of mirror plate has an additional angle, $2\theta_2$, to rotate.

2.3. The characteristic curve between the angular deflection and the driving voltage

The angular deflection θ of the mirror plate for the existing META is determined by the torsional stiffness of the suspension K_t and the torque T_e induced by electrostatic force. The torsional stiffness of the straight type suspension shown in Fig. 4 is [6]

$$K_t = \frac{2Eh_2W_s^3}{L_s} \left[\frac{1}{3} - 0.21 \frac{W_s}{h_2} \left(1 - \frac{W_s^4}{12h_2^4} \right) \right], \quad (3)$$

where E is the elastic modulus, and h_2 , W_s , and L_s are the thickness, width and length, respectively, of the straight suspension.

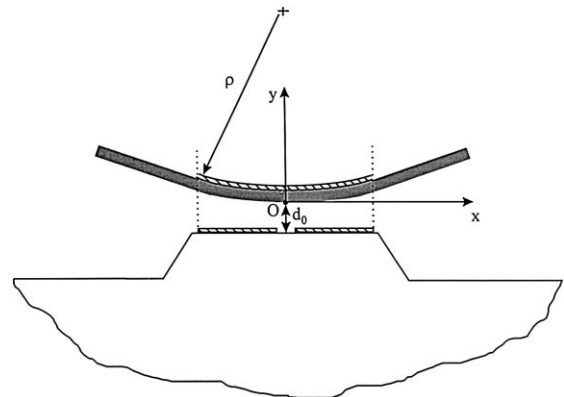


Fig. 6. The gap between the top and bottom electrodes of a partially bent mirror plate.

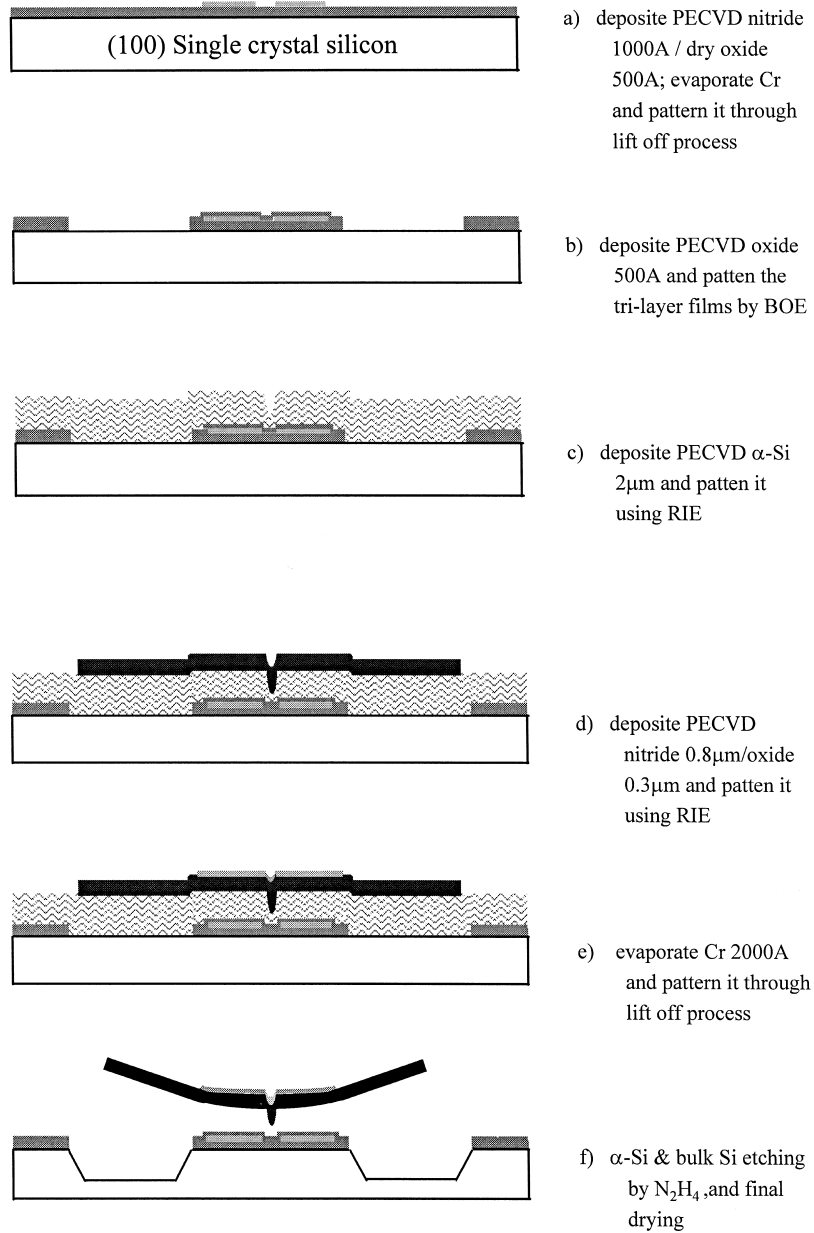


Fig. 7. Fabrication processes of the proposed META.

Note that in this paper, the mirror plate located between the top and bottom electrodes is considered a dielectric layer. Therefore, in analyzing the torque T_e induced by electrostatic force, the effective gap between the electrodes must be modified to

$$d_{\text{eff}} = d_0 + \frac{h_2}{k}, \quad (4)$$

where h_2 and k are the thickness and dielectric coefficient of the mirror plate, respectively. Since the angular deflection is small, T_e is approximated to [6]

$$T_e \approx \frac{\kappa_a W_e V^2}{2\theta^2} \left[\frac{L_e \theta}{d_{\text{eff}} - L_e \theta} + \ln \left(1 - \frac{L_e \theta}{d_{\text{eff}}} \right) \right], \quad (5)$$

where κ_a is the dielectric constant of the air, W_e are the width of the top electrode, and V is the driving voltage.

From Eqs. (3) and (5), the relationship between the driving voltage V and the angular deflection for the typical surface META shown in Fig. 1b becomes

$$V = \left\{ \frac{\frac{4Eh_2W_s^3\theta^3}{\kappa_a L_s W_e} \left[\frac{1}{3} - 0.21 \frac{W_s}{h_2} \left(1 - \frac{W_s^4}{12h_2^4} \right) \right]}{\frac{L_e \theta}{d_0 - L_e \theta} + \ln \left(1 - \frac{L_e \theta}{d_{\text{eff}}} \right)} \right\}^{\frac{1}{2}}. \quad (6)$$

Following Eq. (6), the characteristic curve between the angular deflection θ and the driving voltage V of the surface META shown in Fig. 1b is determined. Shown by

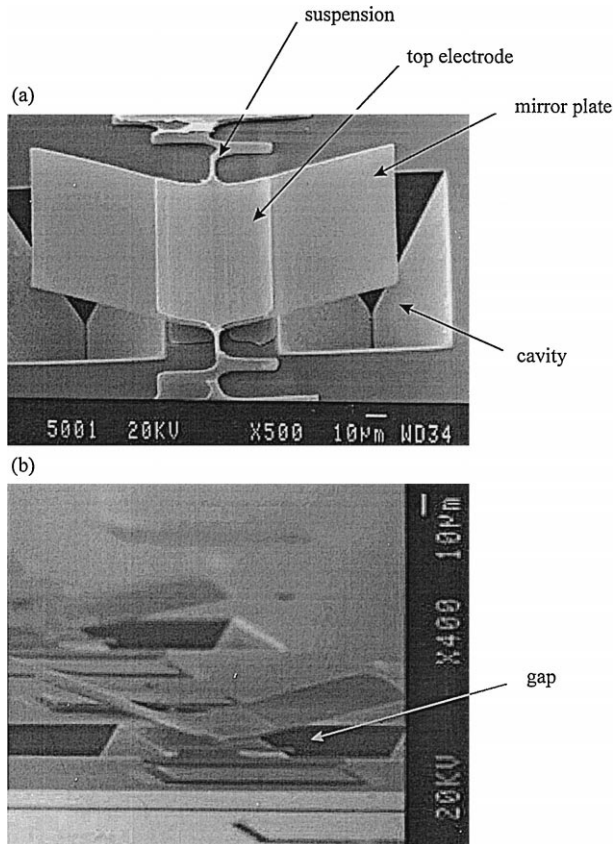


Fig. 8. SEM photographs of a META with partially bent mirror plate: (a) top view and (b) side view.

the solid line in Fig. 5a is a predicted characteristic curve with the electrodes $L_e = 30 \mu\text{m}$ and $W_e = 30 \mu\text{m}$, suspensions $L_s = 80 \mu\text{m}$, $W_s = 2 \mu\text{m}$, and $h_2 = 1 \mu\text{m}$, gap $d_{\text{eff}} = 2 \mu\text{m}$, and $E = 66 \text{ GPa}$. The slope of the characteristic curve will be increased drastically when the mirror plate is under a large driving voltage, and the position of the plate becomes very sensitive to the variations in the driving voltage. In fact, once the driving voltage reaches a critical value V_c , the plate will experience an abrupt tilting until it makes contact with the substrate as shown in Fig. 5b [6].

If the mirror plate with the electrode is bent with a radius of curvature ρ , then the profile of the electrode as shown in Fig. 6 is approximated to

$$y = \frac{x^2}{2\rho} \quad (7)$$

thus the gap between the electrodes is approximately

$$d = \frac{x^2}{2\rho} - \theta x + d_{\text{eff}} \quad (8)$$

and the torque T_e becomes

$$T_e = \int_0^{L_e} \left[\frac{\kappa_a W_e V^2}{2 \left(\frac{x^2}{2\rho} - \theta x + d_{\text{eff}} \right)^2} \right] x dx \quad (9)$$

From Eqs. (3) and (9), the new characteristic curves between the angular deflection and the driving voltage of the META shown in Fig. 5a are obtained. The dash lines displayed in Fig. 5a represent the characteristic curves of partially bent mirror plates with $\rho = 1000 \mu\text{m}$ and $100 \mu\text{m}$. Apparently, the slope of a characteristic curve at a certain angular position for $\rho = 1000 \mu\text{m}$ plate is smaller than that for $\rho = 100 \mu\text{m}$ plate. Hence, the plate with a smaller radius of curvature has a wider operating range. The disadvantage of a partially bent mirror plate META is the increase in the driving voltage, which is due to the increase in the gap between the top and bottom electrodes as shown in Fig. 6.

3. Experiment and results

In order to demonstrate the concept proposed in this study, experiments integrating bulk and surface micromachining processes were conducted. The fabrication processes that contain five masks are shown in Fig. 7. The processes illustrated in Fig. 7a–e are standard surface micromachining and the process shown in Fig. 7f is bulk micromachining. The most critical process in Fig. 7 involves the deposit and pattern of a sacrificial layer on top of the cavity before bulk etching. A bulk-like META is

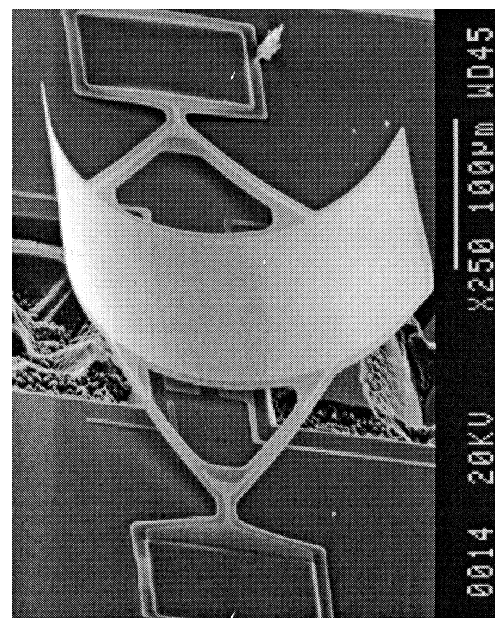


Fig. 9. SEM photograph of a META with fully bent mirror plate.

obtained in Fig. 7f through these processes without the need for a bonding process.

As shown in Fig. 7a–b, the proposed fabrication processes used thermal oxide and plasma-enhanced chemical vapor deposition (PECVD) nitride as the resistant mask to define the area of the cavities. The bottom electrodes were fabricated through lift-off processes and then protected by PECVD TEOS oxide. A 2- μm thick amorphous silicon ($\alpha\text{-Si}$) was deposited by PECVD and then patterned using reactive ion etching (RIE) as shown in Fig. 7c. This layer was the sacrificial layer for surface micromachining. There are two advantages in choosing amorphous silicon as the sacrificial layer. First, the etching solution N_2H_4 has high selectivity between amorphous silicon and the bilayer thin films consisting of PECVD nitride and TEOS oxide. Therefore, the structural layer (mirror plate) formed by the bilayer thin film will not be attacked while removing the sacrificial layer. Second, the bulk etching can be conducted continuously with no requirement to change the etching solution after removing the amorphous silicon sacrificial layer.

As shown in Fig. 7d, the structural layer formed by the PECVD nitride and TEOS oxide was deposited and then patterned using RIE. The TEOS oxide was used to compensate the residual bending moment of the PECVD nitride to maintain the flatness of the mirror plate. After the lift-off processes, the top electrodes were obtained as indicated in Fig. 7e. It is critical to select the properties and dimensions of electrode films in order to determine the angle θ_2 in Fig. 3b. The substrate was etched with a 80% N_2H_4 solution at 85°C . The silicon substrate that was not protected by the resistant mask as illustrated in Fig. 7b will be etched using a N_2H_4 solution after the sacrificial layer has been removed. Finally, the suspensions and mirror plates of the META were suspended, and the auxiliary cavities on the substrate were also formed as shown in Fig. 7f. The dimple in Fig. 8f is used not only to prevent the stiction effect during the drying process, but also to prevent the mirror plate from making contact with the substrate by the electrostatic force induced in driving the actuator.

Fig. 8a is a SEM photograph of a typical META fabricated through the proposed fabrication process. From this photograph, the suspensions, mirror plate, top and bottom electrodes, and auxiliary cavities can be observed. The dimension of the mirror plate is $200\ \mu\text{m} \times 150\ \mu\text{m}$. Fig. 8b is the side view of the META shown in Fig. 8a. It is evident that the mirror plate has a tilting angle with the substrate. This is due to the partially bent effect of the mirror plate discussed in Section 2. It was observed that the phenomenon predicted by the theoretical analysis agrees very well with the experimental observation. In Fig. 9, the entire mirror plate was deposited with electrode film and then bent by the bending moment of the thin films. Thus, the flat area of the mirror plate no longer exists. Measurements using a reflected laser beam to detect the rotation of

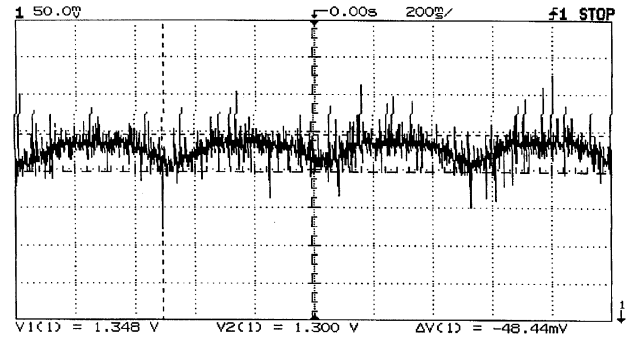


Fig. 10. A typical measured signal of a rotating META from oscilloscope.

the META shown in Fig. 8 were also conducted. The light intensity that varied with the position of the mirror plate was obtained using a photodiode. A typical measured signal from an oscilloscope is shown in Fig. 10. In such a case, the META rotated periodically when it was driven by a sinusoidal input.

4. Discussion

A novel META fabricated through the integration of bulk micromachining and surface micromachining processes was proposed in this paper. The driving voltage of this META is the same as that of a surface META, since the gap between the electrodes is small. However, an auxiliary cavity was etched on the silicon substrate to increase the space between the tips of the mirror plate and the substrate. In addition, the thin film residual stress was exploited to modify the shape of the META. Therefore, the total traveling distance d_{total} of the META can be increased from d_0 to

$$d_{\text{total}} = d_0 + d_1 + L_p \theta_2. \quad (10)$$

Similarly, the total angular deflection θ_{total} can be increased from θ_0 to

$$\theta_{\text{total}} = \theta_0 + \theta_1 + \theta_2. \quad (11)$$

If the desired angular deflection θ_0 remains unchanged, then the length of the mirror plate L_p is increased from d_0/θ_0 to

$$L_p = \frac{d_0 + d_1}{\theta_0 - \theta_2}. \quad (12)$$

The length of the mirror plate can be arbitrarily increased once θ_2 is greater than θ_0 . In short, the proposed META has the following advantages: (1) lower driving voltage, (2) larger allowable angular deflection or larger length of the mirror plate, and (3) no bonding process required.

Since the thin film residual stress is controllable through the fabrication processes, the radius of curvature of a partially bent mirror plate is adjustable. Consequently, the angle θ_2 can be adjusted by residual stress. There is one

more controllable parameter necessary to reach a desired traveling distance, angular deflection, length of mirror plate through Eqs. (10)–(12). In addition, the characteristic curve between the driving voltage and the angular deflection of the proposed META is also controllable through the thin film residual stress. Thus, the performance of the proposed META becomes adjustable and controllable.

Acknowledgements

This material is based (in part) upon work supported by the Mechanical Industry Research Laboratories, Industrial Technology Research Institute (ITRI) and the National Science Council under Grant NSC 86-2221-E007-029. The author would like to appreciate the Electrical Engineering Department of National Tsing Hua University, Semiconductor Center of National Chiao Tung University, and National Nano Device Laboratories in providing the fabrication facilities. The authors would also like to thank Prof. R.S. Huang and Prof. R.-S. Chen for their valuable suggestions.

References

- [1] S.M. Sze, *Semiconductor Sensors*, Wiley, New York, NY, 1994.
- [2] W. Trimmer, *Micromechanical System*, The Third Toyota Conference, 1989, pp. 1–15.
- [3] H. Toshiyoshi, H. Fujita, Electrostatic micro torsion mirrors for an optical switch matrix, *Journal of Microelectromechanical System* 5 (1996) 231–237.
- [4] D. Chauvel, N. Haese, P.A. Rolland, D. Collard, H. Fujita, A micro-machined microwave antenna integrated with its electrostatic spatial scanning, *The Tenth Annual International Workshop on Microelectromechanical System*, 1997, pp. 84–89.
- [5] S.S. Lee, R.P. Ried, R.M. White, Piezoelectric cantilever microphone and micro speaker, *Journal of Microelectromechanical System* 5 (4) (1996) 238–242.
- [6] P. Jaecklin, C. Linder, N.F. de Rooij, Line-addressable torsional micromirrors for light modulator arrays, *Sensors and Actuators A* 41 to 42 (1994) 324–329.
- [7] M.A. Mignardi, Digital micromirror array for projection TV, *Solid State Technology*, July 1994, pp. 63–68.
- [8] V. Markandey, T. Clatanoff, R. Gove, K. Ohara, Motion adaptive deinterlacer for DMD (Digital Micromirror Device) based digital television, *IEEE Transactions on Consumer Electronics* 40 (1994) 735–742.
- [9] H. Toshiyoshi, H. Fujita, T. Kawai, T. Ueda, Piezoelectrically operated actuators by quartz micromachining for optical application, *IEEE Micro Electro Mechanical System Workshop*, Fort Lauderdale, FL, USA, 1993, pp. 133–138.
- [10] E. Obermeier, J. Lin, V. Schlichting, Design and fabrication of an electrostatically driven microshutter, *Tech. Digest, 7th Int. Conf. Solid-State Sensors and Actuators (Transducer '93)*, Yokohama, Japan, June 7–10, 1993, pp. 132–135.
- [11] M.H. Kiang, O. Solgaard, R.S. Muller, K.Y. Lau, Micromachined polysilicon microscanners for barcode readers, *IEEE Photonics Technology Letters* 8 (1996) 1707–1709.
- [12] R.A. Buser, N.F. de Rooij, H. Tischhauser, A. Dommann, G. Stauffert, Biaxial scanning mirror activated by bimorph structures for medical applications, *Sensors and Actuators A* 31 (1992) 29–34.
- [13] N.C. Tien, O. Solgaard, M.-H. Kiang, M. Daneman, K.Y. Lau, R.S. Muller, Surface-micromachined mirrors for laser-beam positioning, *Dig. Tech. Papers, 8th Int. Conf. Solid-State Sensors and Actuators (Transducer '95)*, Stockholm, Sweden, pp. 352–355.
- [14] P. Jaecklin, C. Linder, J. Brugger, N.F. de Rooij, Mechanical and optical properties of surface micromachined torsional mirrors in silicon, polysilicon and aluminum, *Sensors and Actuators A* 43 (1994) 269–275.
- [15] Fischer, H. Graef, W. von Munch, Electrostatically deflectable polysilicon torsional mirrors, *Sensors and Actuators A* 44 (1994) 83–89.
- [16] C.W. Stormont, D.A. Borkhoder, V. Westerlind, J.W. Suh, N.I. Mulef, G. Kovacs, Flexible, dry-released process for aluminum electrostatic actuators, *Journal of Microelectromechanical System* 3 (1994) 290–296.
- [17] W. Chung, J.W. Shin, Y.K. Kin, B.S. Han, Design and fabrication of micromirror supported by electroplated nickel posts, *Sensors and Actuators A* 54 (1996) 464–467.
- [18] Buhler, J. Funk, J.G. Korvink, F.P. Steiner, P.M. Sarro, H. Baltes, Electrostatic aluminum micromirrors using double-pass metallization, *Journal of Microelectromechanical System* 6 (1997) 126–135.
- [19] W. Fang, J.A. Wickert, Determining mean and gradient residual stresses in thin films using micromachined cantilevers, *Journal of Micromechanics and Microengineering* 6 (1996) 301–309.
- [20] Y. Chen, The fabrication and discussion of silicon nitride membranes by chemical vapor deposition, Master thesis, Chiao-Tung University, Hsinchu, Taiwan, Republic of China, 1997.
- [21] S. Timoshenko, Analysis of bi-metal thermostats, *Journal of Optical Society of America* 11 (1925) 233–255.